Nuclear Materials and Energy 39 (2024) 101687

Contents lists available at ScienceDirect

Nuclear Materials and Energy

journal homepage: www.elsevier.com/locate/nme

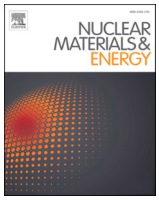

Long-pulse high heat flux testing of tungsten monoblock target mock-ups for investigation of creep fatigue interaction

Gerald Pintsuk [a,*], Emanuele Cacciotti [b], Francesco Crea [b], Daniel Dorow-Gerspach [a], Selanna Roccella [b], Marius Wirtz [a], Jeong-Ha You [c]

[a] Forschungszentrum Jülich GmbH, Institut für Energie- und Klimaforschung – Plasmaphysik, Partner of the Trilateral Euregio Cluster (TEC), 52425 Jülich, Germany
[b] ENEA Fusion and Technologies for Nucl. Safety Dept, C.R. Frascati, C.P.65-00044 Frascati, Rome, Italy
[c] Max Planck Institute for Plasma Physics, Boltzmannstraße 2, 85748 Garching, Germany

ARTICLE INFO

Keywords:
HHF-testing
Electron beam loading
Divertor components
Creep-fatigue

ABSTRACT

Divertor components for ITER and even beyond will be subjected to cyclic steady state heat loads with a duration of several minutes to hours, repeatedly occurring slow transients during reattachment or ramp-up and down, as well as heat loads during ELMs applying a combination of low cycle fatigue and creep as well as high cycle fatigue via thermal shock loads. While for the qualification of components the duration of the fatigue cycles up to now has been kept small, i.e., close to the required time to reach thermal saturation which is 10 s for typical divertor components, creep in these components has not yet been assessed.

In this study divertor tungsten monoblock mock-up manufactured via hot radial pressing in the ITER-like geometry consisting of 4 monoblocks and quality checked via ultrasonic testing are exposed to high heat flux loads in the electron beam facility JUDITH 2 using a high temperature cooling circuit with controlled water chemistry. Thereby, cyclic loads up to 1000 cycles with a duration of 10 to 600 s and a power density of 20 MW/m^2 were applied, representing strike point loading conditions in DEMO during strike point sweeping scenarios. Each of the tungsten monoblocks is loaded individually providing the possibility to study different scenarios on one single mock-up. The aim is to assess the performance and degradation of performance due to the applied loads, which is supported by characterization via metallography, profilometry, SEM and hardness testing after the high heat flux tests.

1. Introduction

Slow transient induced thermal fatigue loads up to 20 MW/m^2 with a duration of 10 s on tungsten divertor components are investigated for a long time [1–5] as potential hazard for ITER and qualification procedures for these components comprise high heat flux testing applying up to 1000 cycles. In a follow up, the same procedures were adopted for the qualification of DEMO divertor components [6] with loads even up to 25 MW/m^2 for 10 s and even higher loads for short cycle durations < 1 s to simulate conditions during off-normal transient events (e.g. plasma reattachment with strike point sweeping) [7]. Thereby, multiple mechanisms for material modification and damage formation were observed including interface delamination, tungsten surface roughening and deformation of the tungsten monoblock [1–5,7]. This can be, due to transient state of the loading achieving steady state like conditions only during the last 1–2 s of the 10 s loading, attributed to fatigue loading only.

However, for DEMO these transient loading conditions can reach durations in the range of some tens of seconds during the mentioned plasma reattachment in order to allow the ramp-down of the plasma current without control losses [8]. This adds to the before mentioned thermal fatigue potentially also an element of creep, in particular at the high occurring temperatures in the individual parts of the component, i.e. the tungsten plasma facing material, the pure Cu interlayer and the CuCrZr cooling tube.

In order to determine, if creep may need to be taken into account superimposed on the existing and known thermal fatigue effects, in this work high heat flux tests with significantly increased cycle duration exceeding the operationally expected duration were performed. In addition, this long-term loading may also provide some insights on the combination of steady state and transient heat loads occurring e.g. during high frequency mitigated edge localized modes (ELMs). This is

* Corresponding author.
E-mail address: g.pintsuk@fz-juelich.de (G. Pintsuk).

https://doi.org/10.1016/j.nme.2024.101687
Received 6 November 2023; Received in revised form 2 June 2024; Accepted 3 June 2024
Available online 4 June 2024

done by taking benefit of the nature of the electron beam with a comparably small beam diameter, which deposits the energy by scanning the surface and thereby locally applies very short thermal shock loads.

2. Test facilities and parameter

The high heat flux tests were performed using the electron beam facility JUDITH 2 [9]. The facility with a maximum power of 200 kW and an acceleration voltage of 40–60 kV provides an electron beam with a Gaussian shape, which is scanned across the surface by means of a digital scanning mode. The minimum duration of each loaded spot in the loading pattern is 5 μs and the beam diameter (at full width half maximum) varies depending on several parameters and in particular on the applied power between 3 and 15 mm. The facility is furthermore equipped with a cooling circuit operating at temperatures from room temperature (RT) to 130 °C, a pressure ≤ 4 MPa and a flow rate ≤ 200 l/min.

The investigated ITER-like monoblock mock-up (see Fig. 1) was produced by ENEA using hot radial pressing (HRP) at a temperature of 580 °C for 2 h. Thereby, a solution annealed, cold-worked and aged (SAcwA) CuCrZr cooling tube with an inner diameter of 12 mm and an outer diameter of 15 mm was joined to a chain consisting of 4 pure tungsten (AT&M. ITER grade tungsten) monoblocks of 23 × 28 × 12 mm each. The tungsten blocks contained an inner borehole of 17 mm diameter and a 1 mm thick pure Cu layer at the inside of this borehole applied via hot isostatic pressing (HIP). The tungsten thickness above the cooling tube was 8 mm and the set distance between the monoblocks was 0.5 mm.

The testing protocol is given in Table 1: Testing protocol Table 1 and the cyclic loading scheme including the total loading time for each particular monoblock is given in Fig. 1. Thereby, the loading scheme with 10 s beam "On" represents is the reference conditions actually used for the qualification of ITER divertor components. While for ITER divertor components the typical investigated cycle numbers are 300 and 1000, due to limited availability of the facility and keeping the pulse durations as set, the lower cycle number for this study was adjusted to 200 arriving at maximum loading time of 33.3 h. The actually used cooling conditions were a flow rate of 97 l/min resulting in a flow

Fig. 1. Monoblock-component before the first screening (top); testing parameters for the individual monoblocks incl. time during beam "On".

Table 1
Testing protocol.

Step	Description
1	Screening of complete chain @ 10 MW/m^2 and 20 MW/m^2
2	Reduction of loaded area to one monoblock, covering others with beam dumps
3	Start screening @ 20 MW/m^2
4	Performing 200 cycles with 10, 300 or 600 s "On", 10 s "Off" or 1000 cycles with 120 s "On", 10 s "Off"
5	Final screening @ 20 MW/m^2
6	Screening of the complete chain @ 10 MW/m^2

velocity of 16 m/s in the mock-up, a coolant temperature of 120 °C and a pressure of 2.6 MPa. The measurement and surveillance of the absorbed heat flux was performed using water calorimetry by determining the increase of the coolant temperature via thermo-couples installed in the coolant loop before and behind the mock-up. Furthermore, the surface temperature is monitored via an infra-red (IR) camera, a two-color pyrometer and a fast one-color pyrometer.

The aim of the tests is the determination, if at the given high thermal loads at the upper operational limit and significantly above the steady state loading conditions for divertor components in ITER and DEMO a potentially life-time limiting interaction of thermal fatigue and creep can be determined affecting the CuCrZr cooling tube and the tungsten/Cu interface. In addition, due to the nature of the electron beam loading, very short (about a factor 100 below the length of an edge localized mode – ELM) thermal shock pulses are applied on the surface at a frequency of 780 Hz. During these pulses, depending on the beam parameters, heat flux factors [10] calculated by $P.t^{1/2}$ with power density P and duration t up to the range of mitigated ELMs can be achieved that may, for recrystallized tungsten, lead to high cycle fatigue induced surface damage. This may provide an additional insight on the performance of tungsten and in particular the tungsten surface in the strike point area of the divertor.

Component qualification before and after testing is done first by ultrasonic testing (UT) to determine the integrity of the component and the interface quality. In a second step, light microscopy, scanning electron microscopy (SEM) imaging and laser profilometry of the tungsten surface was performed to qualify and quantify the material modification. Finally, metallographic investigations also taking the findings from ultrasonic testing into account were aiming to determine the recrystallization in tungsten and potentially occurring bulk and interface damage not detected by surface inspection and non-destructive methods. Subsequent hardness tests in particular in the region of the cooling tube should quantify the effect of microstructural modifications in the higher temperature region close to the individual interfaces.

3. High heat flux testing and damage qualification

3.1. Infra-red monitoring and ultrasonic testing

The shown IR-images during the initial and the final screening of all 4 monoblocks at 10 MW/m^2 (see Fig. 2) indicate first, that there is a certain variation in the thermal performance of the individual monoblocks. Assuming an almost homogeneous surface emissivity with only minor differences related to the manufacturing induced surface finish (cf. Fig. 1), the best performance in cooling capacity before thermal cycling is provided by block #4 showing the lowest average surface temperature. However, the standard deviation of the surface temperature among these 4 blocks at 10 MW/m^2 amounts only to ~ 2.5 % and in addition, the outer blocks are characterized by slightly higher radiation losses due to the additional open surface.

After thermal loading and taking into account that there have been no differences in the cool-down behavior found, as indicated in Fig. 3, the reason for the increase of the measured surface temperature for all 4 monoblocks and in particular blocks #2–4 (see Fig. 2, bottom) should be

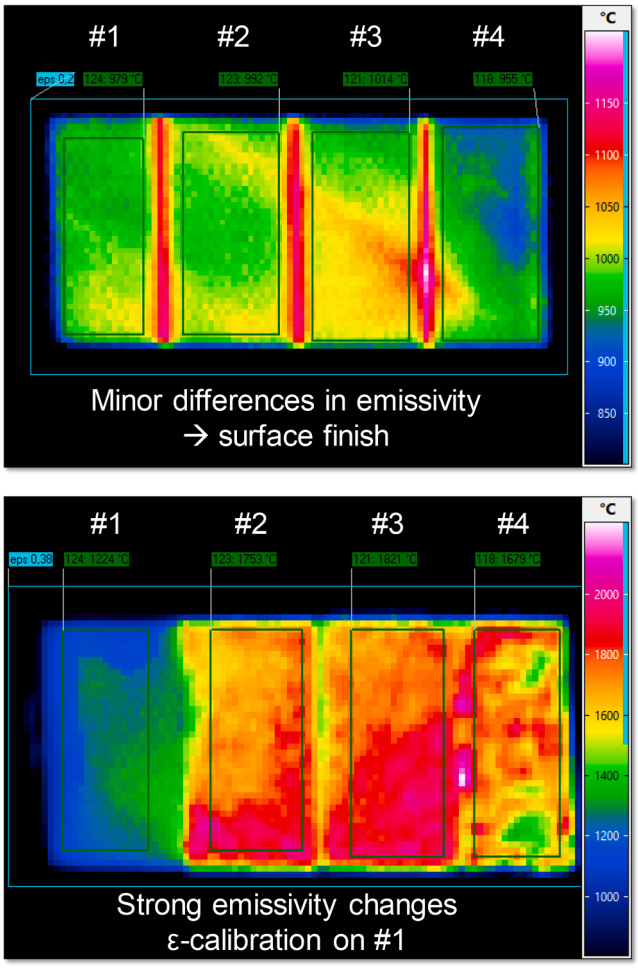

Fig. 2. IR-images during the 10 MW/m^2 screening before (top) and after (bottom) high heat flux testing.

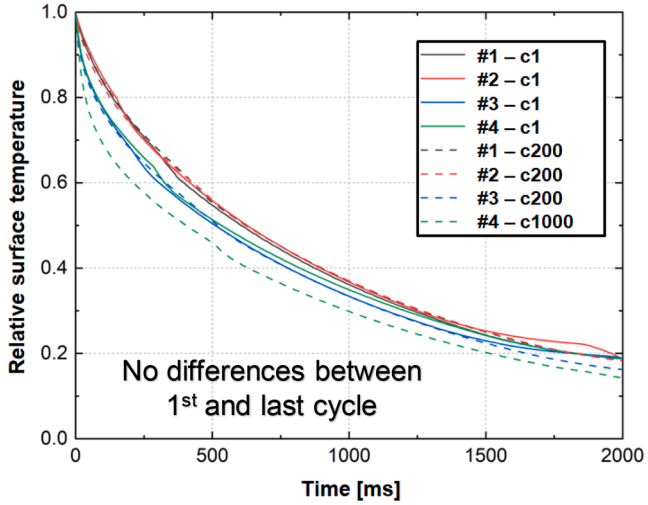

Fig. 3. Cool down performance determined via one-color fast pyrometer after first and last cycle at 20 MW/m^2 normalized on the maximum surface temperature of each individual monoblock.

related to an increase in surface emissivity. This is confirmed by the optical appearance of the mock-up as shown in Fig. 4 indicating the formation of surface structures and a related change in surface roughness that will be investigated and quantified in section 3.2. During

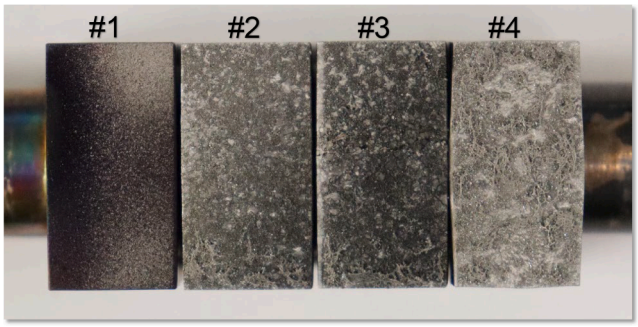

Fig. 4. Monoblock-component after testing showing surface modifications and some "barreling" for #4.

testing, the emissivity setting for the IR-camera was adjusted to the temperature measurement of the two-color pyrometer. While at the beginning the emissivity varied between ~ 0.37–0.42 for the individual blocks, during testing this increased for block #2, #3 and #4 to ~ 0.62.

In addition to the surface modification, only for block #4 and therefore directly related to the higher applied number of cycles, also a change of the monoblock shape has taken place. This is a known effect also shown in [7] and typically identified as "barreling", i.e., a widening of the block in the center along the cooling tube direction, causing a closure of the gap between the blocks #3 and #4. This result gives a first indication, that the applied number of cycles, i.e. thermal fatigue, has a stronger effect on the component and related materials than the loading time and related creep effects, at least for the applied maximum loading duration of 33.3 h.

For further qualification of the mock-up, UT after high heat flux loading has been performed and compared to investigations performed after manufacturing (see Fig. 5). While after manufacturing there were no defects found in the bulk materials as well as the interface between tungsten and the casted pure Cu interlayer, some defects were present at the CuCrZr/Cu-interface. While for block #1 two smaller voids were found in the area directly below the plasma facing surface (180° at the y-axis in Fig. 5) and close to the outer edge, for block #4 a larger area also situated at the outer edge of the block is affected. The damage extends from the center directly below the plasma facing surface almost in a full half circle down to the backside with a maximum damage at about an angle of 45° from the center.

After high heat flux loading changes, similar to after manufacturing, occurring damages are limited to the CuCrZr/Cu-interface. The main affected areas are at the edges between the different monoblocks and there in particular between blocks #1 and #2 as well as between blocks #3 and #4. Furthermore, the existing damage at the outer edge of block #4 increases, e.g. by motion of the crack front by ~ 1 mm towards block #3 at the angle of maximum damage. Under these boundary conditions and despite the fact that the damage is not directly below the loaded surface, the before mentioned best performance of block #4 from the beginning is still a surprising result requiring further analyses.

3.2. *Surface investigations*

In Fig. 6 the surface area and the related surface roughness is provided showing a significant increase of the average surface roughness by a factor of up to ~ 12 with increasing loading time at constant cycle number. At the outer edges of blocks #2 and #3, exhibiting the furthest distance to the cooling tube and accordingly the highest surface temperature, the local surface roughness has been found to be even higher by a factor of ~ 2.

The results for 200 cycles show a fast increase in damage from 10 to 300 s cycle duration, which slows down when further increasing to 600 s cycle duration but not yet reaching a saturation value. This damage may be a combination of low cycle fatigue (LCF) as shown in [7], creep as

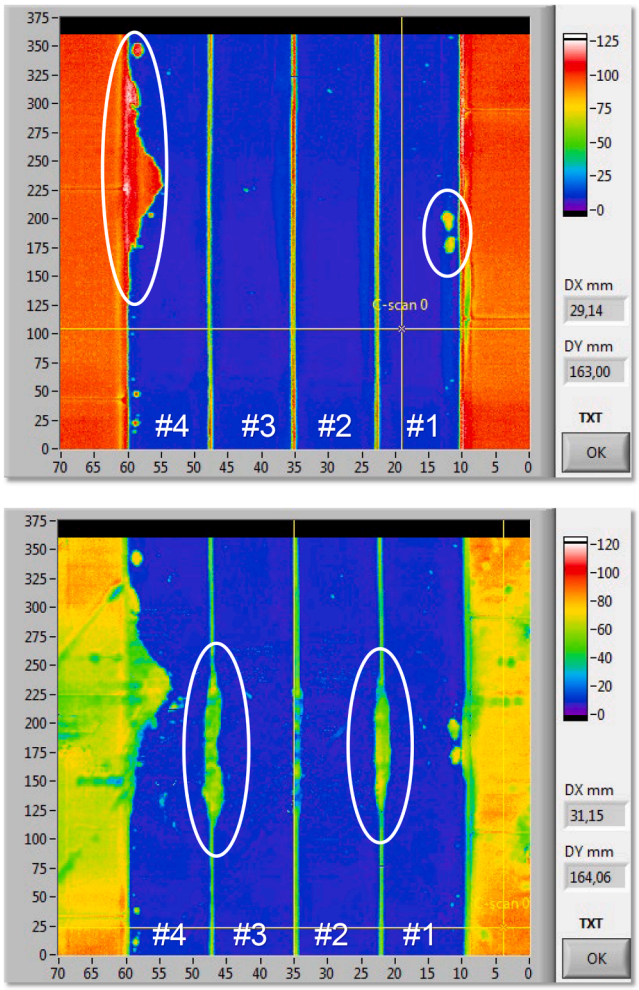

Fig. 5. Ultrasonic testing before (top) and after (bottom) high heat flux testing showing the HRP-interface between Cu and CuCrZr; indicated are manufacturing defects (top) and high heat flux induced defects (bottom).

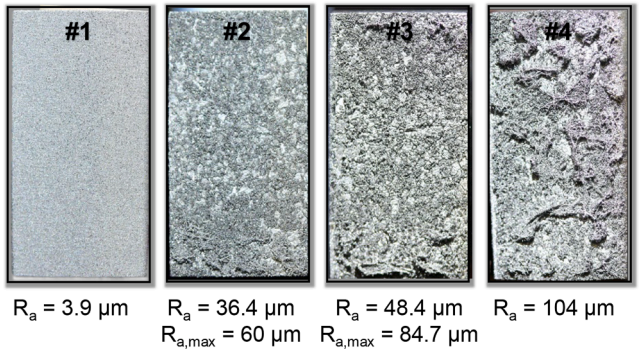

Fig. 6. Light microscopy surface images of the individual monoblocks including average surface roughness R_a and maximum surface roughness $R_{a,max}$ at the edges for #2 and #3.

well as thermal shock induced high cycle fatigue (HCF). The boundary condition for the latter were that during electron beam loading with an applied power of ~ 80 kW and a beam diameter of ~ 8 mm, 1.56×10^6 (block #1) to 93.6×10^6 (blocks #3 and #4) thermal shock pulses were applied and the measured local temperature increase was 30–50 °C measured by the fast one-color pyrometer with a time resolution of 10 µs. Calculating for a temperature rise of 50 °C the absorbed power density using formula (3) from [11] with power density P, duration t, thermal conductivity λ, density ρ and heat capacity c:

$$\Delta T = 2P\left(\frac{t}{\pi\lambda\rho c}\right)^{1/2} \quad (1)$$

and using material data for an assumed surface temperature of 2000 °C during thermal cycling at 20 MW/m^2 (λ = 96 W/m.K, c_p = 182.8 J/kg, ρ = 19.22 g/cm^3) this amounts to ~ 364 MW/m^2. This further translates into a heat flux factor FHF = ~0.81 MW/m^2*s$^{1/2}$, which is well below the minimum value of ~ 3 MW/m^2*s$^{1/2}$ that was yet used for dedicated ELM simulations in JUDITH 2 and which was found to be above the damage threshold for recrystallized tungsten. Assuming further that the electron beam is characterized by a perfect Gaussian shape so that 76 % of the energy are deposited within the FWHM and furthermore taking the electron absorption coefficient of tungsten of 0.55 into account, the electron beam diameter during loading would have needed to be about 10.5–11 mm in diameter. That would have been significantly larger than the initially determined value which would have resulted in an FHF = 1.49 MW/m^2*s$^{1/2}$.

In any case, without having explicit experimental data for these loading conditions, this is highly likely to be sufficient to result in surface damage like roughening and micro-crack formation, which is confirmed by the cracking pattern of individual grains and the loss of particles shown for block #1 in Fig. 7. HCF is most likely also the main reason for the increase in surface damage and, in particular, the fine damage structures by increasing the loading time. However, the further roughness increase on block #4 (1000 cycles) by another factor of ~ 2 compared to block #3 (200 cycles) is clearly related to the steady state cycles and accordingly low cycle fatigue (LCF), both experiencing the same total loading time and number of thermal shock induced loads. This effect and its extension was unexpected, in particular when looking at the found fine microstructural features shown for block #4 in Fig. 7.

3.2. Metallographic investigations

Metallographic cross sections of each monoblock perpendicular to the cooling tube show in Fig. 8 the recrystallization depth in tungsten in the center of the block. Similar to the evolution of surface roughness and as expected from tungsten recrystallization kinetics [12], there is a significant increase in recrystallization depth due to the increase of loading time from block #1 to block #2 including the onset of secondary recrystallization at the top surface forming huge tungsten grains in the mm-range. The further increase of loading time for block #3 leads to a further but comparably marginal increase in recrystallization depth. However, block #3 contains a macro-crack extending almost through the full thickness of the tungsten block down to the W/Cu-interface, which was not visible from the top surface and due to the direction of the crack not or hardly visible by UT done typically from inside the cooling tube. The formation of the macro-crack is remarkable as this damage mode is not typical/seldom for this kind of tungsten material and normally only seen in past experiments for larger geometries with 28 mm wide tungsten blocks as used for the ITER divertor.

For block #4, in contrast to block #3 experiencing the same loading time, a significantly reduced recrystallization depth and also lower amount of secondary recrystallization was found. This might be on the one hand related to a better cooling efficiency, which were shown already by the initial thermal screening results at 10 MW/m^2. On the other hand, the formation of the observed surface structures might play a role as the loading of these structures showing a reduced thermal transfer via the electron beam would result in surface overheating and a related lower heat penetration depth into the bulk material. However, the latter explanation does not correspond to the determined lower temperature of block #4 during final screening at 10 MW/m^2 (see Fig. 2.

Looking at the W/Cu-interface via UT a small defect was found in block #3 in the center, i.e. directly below the thermally loaded surface

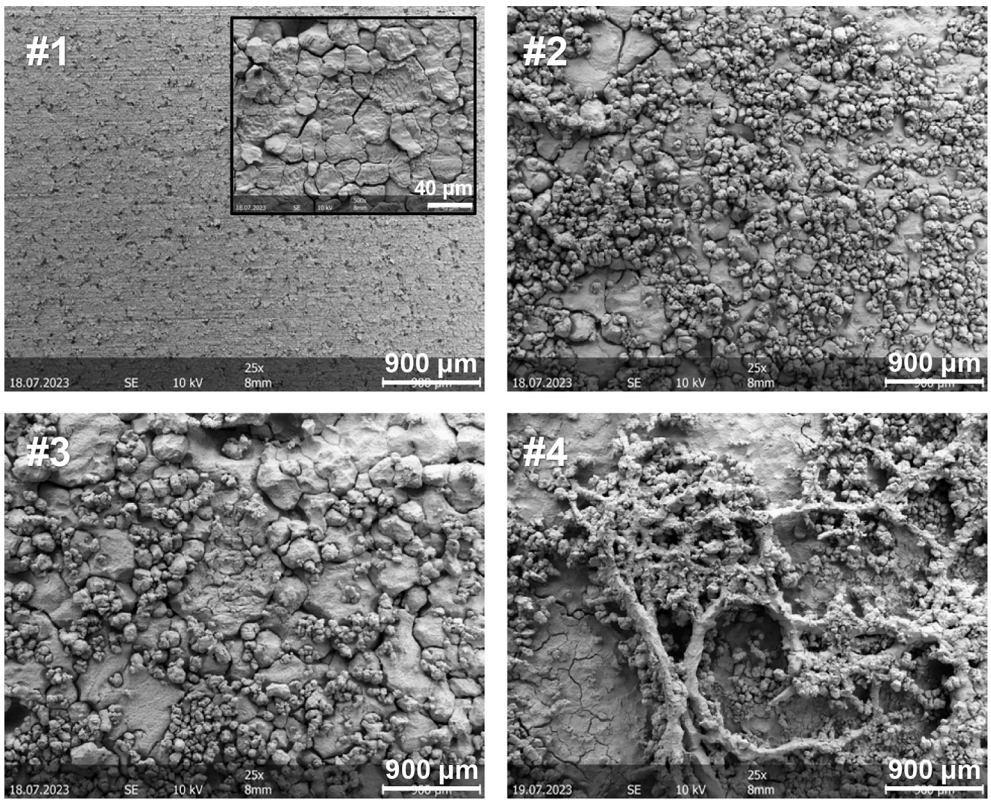

Fig. 7. SEM images of the individual monoblocks.

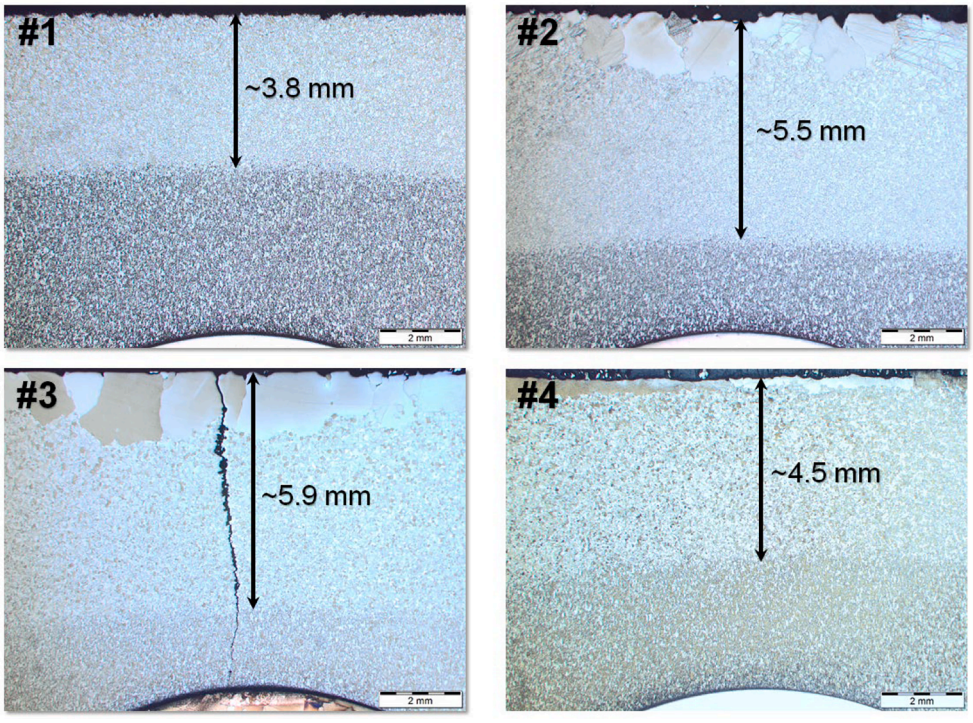

Fig. 8. Metallographic cross-sections from the plasma facing surface to the cooling tube with indicated recrystallization depth.

and confirmed by metallographic inspection (see Fig. 9). The formation mechanism of this small defect with a shape that would hint more to a casting void after manufacturing than a high heat load induced defect is yet still unclear. However, while the defect seems to be a few mm long, the lateral extension of the defect is very small (~100 µm) and is therefore not expected to have influenced the performance of the component.

Finally, in Cu as well as CuCrZr microstructural modifications in terms of grain growth and grain formation were observed towards the higher temperature region in both materials. Investigating the hardness

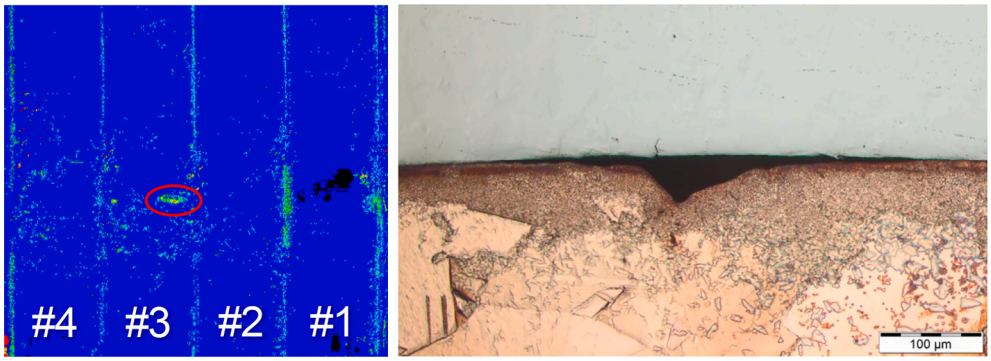

Fig. 9. Ultrasonic testing results at the W/Cu-interface and related metallographic cross section at the defect location.

of Cu and CuCrZr in the area directly below the loaded surface shows that for Cu the hardness is the same for blocks #1 to #3 and is lower for block #4 (see Fig. 10). As the only common difference between those blocks is the number of applied cycles, the reason might be an increased accumulated plastic compressive strain under loading and consequently higher residual tensile stresses in Cu. For CuCrZr the situation is more complex as the hardness at the outer monoblocks seem to vary from those of the inner blocks already after manufacturing, i.e. for the outer ones a hardness > 100 HV0.5 and for the inner < 90 HV0.5. There is an indication that a higher loading time reduces the hardness, but without having the data directly after manufacturing, no conclusion can be drawn yet despite that this effect needs to be taken into account in the evaluation of future test results in case of potential differences between inner and outer tiles.

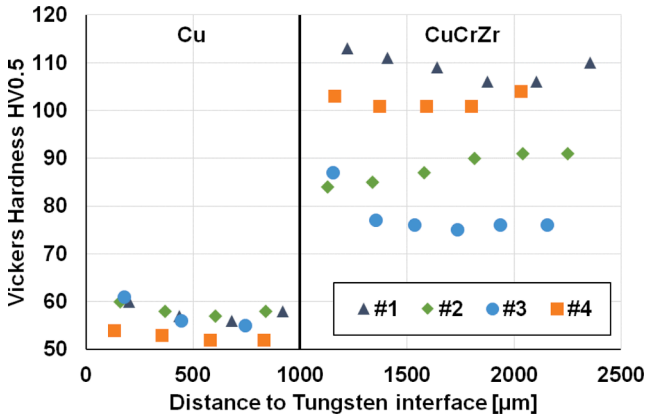

Fig. 10. Hardness testing in Cu and CuCrZr for all monoblocks after high heat flux testing.

4. Summary and conclusions

The investigation of a tungsten monoblock mock-up was performed using on the one hand high heat flux testing with constant cycle number and increasing cycle duration and on the other hand an increase in cycle number with constant maximum loading time. This aims at the determination if in addition to thermal fatigue also creep effects have to be taken into account for the lifetime evaluation. The resulting modifications of the component were analyzed by non-destructive and destructive means leading to the following conclusions:

- No performance degradation of the component was found due to the combined creep/fatigue loading although an onset of interface degradation at the HRP-interface (Cu to CuCrZr) was found to occur close to the gaps between different blocks extending along the cooling tube direction.
- Extensive surface roughening was found to be most probably a combination of high (ELM-like) and low (steady state) cycle fatigue as it could be expected for the strike point region of the divertor.
- Increased loading duration at constant cycle numbers increases the recrystallization depth for all investigated blocks except for block #4, which might be related to a better cooling efficiency connected to larger thermal radiation losses or, less likely, the formation of the observed surface structures showing a reduced thermal transfer and therefore a lower heat penetration depth and requires further investigation.
- The formation mechanism of the small defect found only after testing by UT and metallography at the W/Cu-interface in block #3 with a shape normally observed after manufacturing is yet still unclear. However, this kind of defect is not expected to jeopardize the performance of the component.
- Macro-crack formation was detected once, which is not typical for the small block geometry with 23 mm width. If this is a recurrent problem would require better statistics and accordingly a larger sample number. However, the crack did not show any obvious influence on the performance of the mock-up.

In conclusion, based on the actual results thermal fatigue is the dominating damage mechanism. The influence of creep on surface degradation could not yet completely excluded but for the stability of the CuCrZr/Cu cooling structure and the integrity of the various interfaces it has no substantial effect, at least for the given maximum loading time applied here.

CRediT authorship contribution statement

Gerald Pintsuk: Writing – original draft. **Emanuele Cacciotti:** Investigation. **Francesco Crea:** Investigation. **Daniel Dorow-Gerspach:** Methodology, Investigation, Data curation. **Selanna Roccella:** Supervision, Resources. **Marius Wirtz:** Supervision. **Jeong-Ha You:** Supervision, Resources, Project administration, Formal analysis.

Declaration of competing interest

The authors declare that they have no known competing financial interests or personal relationships that could have appeared to influence the work reported in this paper.

Data availability

Data will be made available on request.

Acknowledgments

This work has been carried out within the framework of the

EUROfusion Consortium, funded by the European Union via the Euratom Research and Training Programme (Grant Agreement No 101052200 — EUROfusion). Views and opinions expressed are however those of the author(s) only and do not necessarily reflect those of the European Union or the European Commission. Neither the European Union nor the European Commission can be held responsible for them.

References

[1] S. Panayotis, et al., Fracture modes of ITER tungsten divertor monoblock under stationary thermal loads, Fusion Eng. Des. 125 (2017) 256–262.
[2] M. Fukuda, et al., Performance evaluation of tungsten for ITER divertor toward mass production, Fusion Eng. Des. 167 (2021) 112283.
[3] Z. Sun, et al., Post examination of tungsten monoblocks subjected to high heat flux tests of ITER full-tungsten divertor qualification program, Fusion Eng. Des. 121 (2017) 60–69.
[4] K. Ezato, et al., Development of tungsten divertor components for ITER in Japan, Fusion Eng. Des. 136 (2018) 683–689.
[5] P. Gavila, et al., High heat flux testing of EU tungsten monoblock mock-ups for the ITER divertor, Fusion Eng. Des. 98–99 (2015) 1305–1309.
[6] J.H. You, et al., Diverter of the European DEMO. engineering and technologies for power exhaust, Fusion Eng. Des. 175 (2022) 113010.
[7] J.H. You, et al., High-heat-flux performance limit of tungsten monoblock targets. impact on the armor materials and implications for power exhaust capacity, Nuclear Materials and Energy 33 (2022) 101307.
[8] M. Siccinio, et al., Impact of the plasma operation on the technical requirements in EU-DEMO, Fusion Eng. Des. 179 (2022) 113123.
[9] P. Majerus, et al., The new electron beam test facility JUDIHT II for high heat flux experiments on plasma facing components, Fusion Eng. Des. 75–79 (2005) 365–369.
[10] J. Linke, High heat flux performance of plasma facing materials and components under service conditions in future fusion reactors, Fusion Sci. Technol. 49 (2006) 455–464.
[11] T. Hirai, et al., Thermo-mechanical calculations on operation temperature limits of tungsten as plasma facing material, Fusion Eng. Des. 82 (2007) 389–393.
[12] T. Larsen, et al., Thermal stability of differently rolled pure tungsten plates in the temperature range from 1125 °C to 1250 °C, Fusion Eng. Des. 192 (2023) 113581.